BMC Oral Health

RESEARCH

Open Access

In vitro evaluation of the effects of various remineralization agents on root caries

Merve Sahin[1*], Dina Erdilek[2] and Nursen Topcuoglu[3]

Abstract

Introduction Although various additions are made to fluoride varnishes, there is limited research on their effects on the root caries.

Objective This study compared the effects of different fluoride varnishes on artificial root caries lesions and biofilm formation.

Methodology Bovine root dentin specimens were prepared and demineralized. Specimens were randomly allocated to six groups (n=23/group): (1) Untreated control; (2) Sodium Fluoride (NaF); (3) NaF+ Casein Phosphopeptide-stabilized Amorphous Calcium Phosphate complexes (CPP-ACP); (4) NaF+ Tricalcium Phosphate (TCP); (5) NaF+ Xylitol-coated Calcium and Phosphate (CXP); and (6) Silver Diamine Fluoride/Potassium Iodide (SDF/KI). Specimens (n=15) for spectral analysis were subjected to pH cycling. Before and after pH cycling, FTIR-ATR and laser fluorescence (LF) were used to detect changes in organic/inorganic content. *S. mutans* and *L. casei* dual-species biofilm were performed on artificial caries lesions treated with remineralization agents (n=8). Bacterial biofilm formation was evaluated with CLSM and SEM.

Results According to the laser fluorescence results, SDF/KI showed maximum remineralization values. All treatments reduced LF values compared with control group. FTIR-ATR showed SDF/KI–specific post-cycling bands (weak C = O at ~ 1735–1740 cm^{-1} and a subtle ~ 1090–1095 cm^{-1} shoulder), while phosphate/amide I ratios in NaF, CPP-ACP, TCP, and CXP varnish groups decreased after cycling but tended to remain higher than control, with no differences among varnishes ($p > 0.05$); ratios were not calculated for SDF/KI. CLSM analysis showed that all varnishes are effective on total and viable biomass. However, NaF was the most effective material preventing biofilm formation. The application of varnishes reduced biofilm formation and demineralization of root caries.

Conclusion Within the limits of this study, fluoride varnishes were found to be beneficial in preventing further demineralization of root tissues.

Keywords Root caries, Remineralization, FTIR-ATR, CLSM, SEM

*Correspondence:
Merve Sahin
merve.sahin@kent.edu.tr
[1]Department of Restorative Dentistry, Faculty of Dentistry, Istanbul Kent University, Siraselviler St. No:71 Cihangir, Beyoglu, Istanbul 34433, Turkey
[2]Independent Researcher, Istanbul, Turkey
[3]Department of Basic Medical Sciences, Faculty of Dentistry, Istanbul University, Istanbul, Turkey

Introduction

Root caries are very common cases in elderly patients, and the prevalence of root caries has been reported to be 41.5% worldwide in recent studies [1, 2]. Unlike enamel caries, root caries develop on cementum and dentin, which are more susceptible to demineralization due to their lower mineral content and higher organic composition [3, 4].

Moreover, restorative procedures for root caries present challenges, such as weak bonding of adhesives to dentin, high stress concentration in cervical areas, and difficulty in subgingival isolation [5]. Therefore, non-invasive strategies aimed at preventing or reversing root caries in its early stages are crucial.

Fluoride varnishes are widely used for caries prevention, and recent formulations incorporate additional agents—such as silver ions, phosphoproteins, protease inhibitors, hydroxyapatite precursors, and sugar alcohols—to enhance remineralization efficacy [6]. However, most studies evaluating these agents focus on enamel rather than root caries, and the effectiveness of these formulations on dentin and cementum remains unclear.

Previous research has investigated 5% sodium fluoride (NaF) varnish, as well as the addition of remineralization agents such as Casein Phosphopeptide-stabilized Amorphous Calcium Phosphate (CPP-ACP) and Tricalcium Phosphate (TCP), but studies on their effects on root caries are limited. Furthermore, to our knowledge, no studies have assessed the impact of Xylitol-coated Calcium and Phosphate (CXP™) on root surfaces. Additionally, while Silver Diamine Fluoride (SDF) is highly effective in preventing and arresting root caries, its major drawback is the discoloration it causes [2, 7]. The introduction of a two-step varnish system (Riva Star), which includes the application of potassium iodide (KI) after SDF, aims to reduce this discoloration, but its effectiveness in maintaining remineralization potential while minimizing staining remains unclear.

Given these gaps in the literature, this study aims to evaluate the effects of various fluoride varnishes on artificial root caries lesions by assessing their impact on chemical composition, mineralization, and biofilm formation. The findings will provide insights into the relative efficacy of these agents, offering valuable data for optimizing preventive strategies in managing root caries. The study tested the null hypothesis (H_0) that SDF/KI, NaF, NaF + CPP-ACP, NaF + TCP, and NaF + CXP do not differ in their effects on remineralization and biofilm outcomes; the alternative (H_1) anticipated at least one inter-group difference.

Materials and methods

Ethics approval

As only animal by-products were used and no procedures were performed on live animals, formal ethical approval was not required. Ethical approval for the saliva sample was obtained from the Istanbul University Faculty of Dentistry, Non-Interventional Clinical Research Ethics Committee (File no: 2019/63; Decision no: 88; Date: 11/07/2019).

Sample preparation

Fifty non-carious maxillary bovine incisors from cattle aged 12 and 24 months were obtained from animals slaughtered for commercial purposes at Istanbul Meat&Food Marketing Industry Trade Company (Istanbul, Turkey). An a priori power analysis was conducted in G*Power 3.1 with $\alpha = 0.05$, power = 0.80, and a medium effect size ($f = 0.30$) indicating a required sample of ≈20 per group. For biofilm endpoints a sensitivity analysis showed that with $n = 8$ per group the smallest detectable effect was $f \approx 0.55$ ($\eta^2 \approx 0.23$), corresponding to a large effect.

Extracted teeth were inspected to confirm the absence of caries or cracks and stored in 0.1% thymol at 4 °C for 7 days prior to specimen preparation. Given our 1-week storage, no meaningful impact on dentin properties or remineralization read-outs is expected; reported composition/FTIR shifts are mainly associated with longer storage durations [8]. Based on published data, short-term storage in 0.1% thymol (≤ 2 months) does not meaningfully affect enamel/dentin properties; adverse changes are mainly associated with long-term storage. Specimens were rinsed with distilled water before DIAGNOdent and FTIR measurements to minimize any residue-related artefacts. A low-speed diamond saw was used to produce blocks with cementum and underlying dentin tissue (Isomet, Buehler Ltd, Evanston IL, U.S.A.).

From each tooth, 2-mm dentin slices were prepared. The cementum surfaces of the samples were polished using 600, 800, and 1200 grits of abrasive paper discs (Al_2O_3) (Allied High Tech Product Inc., Comptom, CA, U.S.A.) in a polishing device (Buehler MetaServ 250 Grinder-Polisher, Buehler, Düsseldorf, Germany). Each slice was sectioned into six blocks (4 × 4 × 2 mm), yielding 138 blocks in total (23 teeth; six blocks per tooth). If stereomicroscopic examination (Olympus ZS61, Olympus Corporation, Tokyo, Japan (× 25) revealed a crack or other defect in any block, all six blocks from that slice were excluded. Subsequently, the samples were embedded in acrylic resin (Blaucryl, Efes Dental, Izmir, Turkey) [9]. In order to remove the smear layer, the samples were kept in distilled water in an ultrasonic cleaning device (Digital Ultrasonic Cleaner, Codyson, China) for 5 minutes [10].

Experimental design

Laser fluorescence (LF) measurements were made with DIAGNOdent 2095 (KaVo, Germany). D1 values were obtained by recording the values observed following the measurements, taking into account the codes on the samples. Ninety samples with a Diagnodent score between 10–15 were reserved for spectral analysis.

Formation of artificial caries lesion

Artificial caries lesions were created in all 138 samples. Demineralization solution was prepared with a content of 50 mM acetic acid, 1.5 mM $CaCl_2$, 0.9 mM KH_2PO_4(monopotassium phosphate). The solution was adjusted to pH 5 by the addition of KOH (potassium hydroxide). Solutions were freshly prepared and replaced daily. All samples were kept at 37 °C for 5 days in chambered containers containing 20 ml of demineralization solution for each. After removal from the solution, the samples with artificially induced caries lesions were rinsed with deionized water and stored in deionized water under humid conditions for 24 h [10].

Table 1 Varnishes used in the study

Varnish	Active ingredient	Instruction to use	Manufacturer and Lot Number
Sterile Deionized Water (W)	Chlorine, ammonium, sulfate, magnesium, calcium, sodium (< 2 ppm)		-
Proshield Varnish (P)	Sodium fluoride (5%), resin, ethanol, xylitol	Apply varnish thinly with a brush	President Dental, Germany PD0301B0
MI Varnish™ (M)	Sodium fluoride (5%), CPP-ACP, polyvinyl acetate, ethanol, hydrogenated resin, silicon dioxide (1–5%), sweetener (strawberry/mint flavor)	Open the unit-dose container and stir the varnish with the disposable brush to ensure uniformity. Apply a thin, uniform layer to the teeth.	GC Corp., Tokyo, Japan 2001091
Clinpro™ (C)	Sodium fluoride (5%), tricalcium phosphate (TCP), pentaerythritol glycerol esters of natural resin, ethyl alcohol, water, xylitol, sweetener	Thoroughly mix the varnish with the provided brush. Apply a thin layer to the teeth using sweeping horizontal strokes.	3 M ESPE, U.S.A NA54925
Embrace™ Varnish (E)	Sodium fluoride (5%), xylitol coated calcium phosphate (CXP™), hydrogenated resin, ethanol, silica	Open the varnish pack and dispense the contents. Using the provided brush, apply a thin coat to the teeth with a single horizontal swipe.	PULPDENT Corp., U.S.A 191115
Riva Star (RS)	Step 1: silver fluoride 35–40%, ammonia solution 15–20% Step 2: potassium iodide	Apply Step 1 solution to treatment site. Immediately after, apply a generous amount of Step 2 solution.	SDI, Australia 1146377

Application of remineralization agents

The teeth were divided into a control group (W) plus five experimental groups, with 23 samples in each group. Experimental groups: Sodium fluoride (NaF), Sodium fluoride + Casein Phosphopeptide Amorphous Calcium Phosphate (CPP-ACP), Sodium fluoride + Tricalcium Phosphate (TCP), Sodium fluoride + Xylitol coated Calcium Phosphate (CXP), Silver Diamine Fluoride/Potassium Iodide (SDF/KI) (Table 1). Remineralization agents were applied according to the manufacturers' recommendations.

While 15 samples from each group were used for spectral analysis, 8 samples were kept for use in microbiology analysis. The spectral analysis flowchart of the study is given in Fig. 1.

pH cycling for dentine demineralization

Demineralization solution consists of 50 mM acetic acid, 0.9 mM KH_2PO_4, 1.5 mM $CaCl_2$; pH was adjusted to 5.0. Remineralization solution consists of 20 mM 4-(2-hydroxyethyl)–1-piperazineethanesulfonic acid (HEPES), 1.5 mM $CaCl_2$, 0.9 mM KH_2PO_4, 150 mM KCl; pH was adjusted to 7.0.

The 30-min demineralization and 10-min remineralization durations were selected to model intermittent oral acid challenges rather than net-remineralization conditions, following the pH-cycling approach [11]. This cycle was repeated with 2-h intervals throughout the day so that samples were subjected to pH changes six times a day at room temperature. Then samples were kept in deionized water at + 4 °C overnight. The pH cycle was applied for eight days with freshly prepared solutions that were changed daily [11].

Laser fluorescence measurements

Before use, it was ensured that there were no acrylic residues on the tooth surfaces. All surfaces were lightly dried for 10 s with air–water spray to ensure humidity standardization.

Type B fiber optic tip (probe B) of a DIAGNOdent device designed for flat surfaces was used. Before each measurement, the system was calibrated with the ceramic standard scale on the side of the device following the manufacturer's recommendations.

After calibration, baseline laser fluorescence was recorded by acquiring three readings from a 4 × 4-mm tooth section; the mean of the three readings was used for analysis. During each measurement, the type-B probe

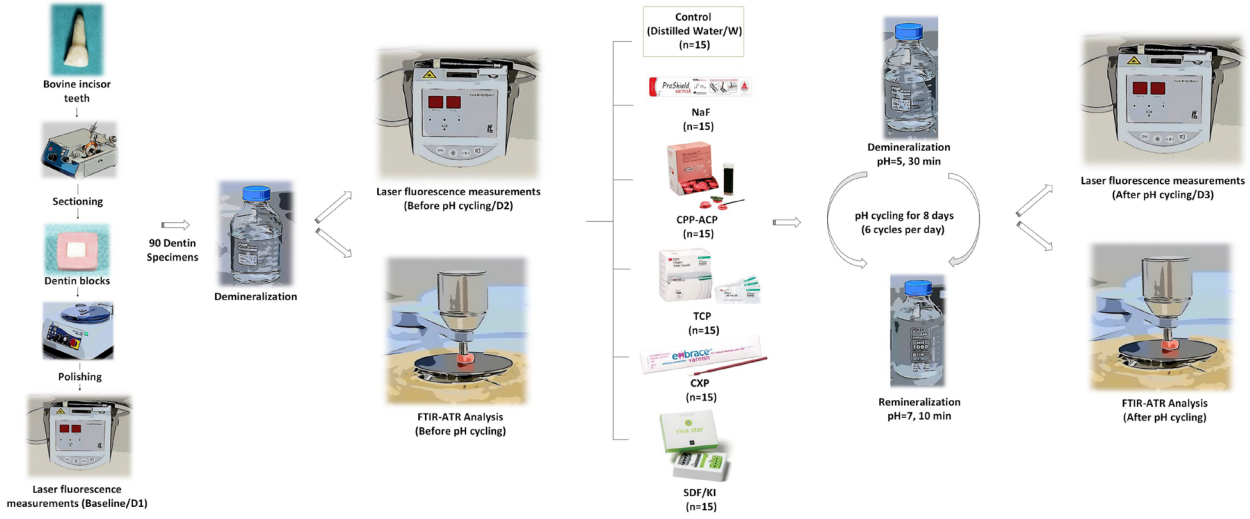

Fig. 1 Flowchart of spectral analysis

was kept in close contact with the surface and gently tilted to collect fluorescence from all directions, as previously described [12]. The initial fluorescence values (D1) of the samples, after demineralization (D2), and post-pH cycle (D3) values were all recorded using the same method.

FTIR-ATR analysis

Five samples from each group were analyzed using the Attenuated Total Reflectance (ATR) unit with a diamond crystal tip of the Spectrum 100 (Perkin Elmer, U.S.A.) before pH cycling.

Prior to examination, the samples were washed with distilled water for 30 s and air-dried. By marking three reference points on each sample, measurements were made in the same position before and after remineralization. The working parameters were determined as 4000–450 cm^{-1} scanning range, 4 cm^{-1}resolution, and 32 scanning frequency. In the current study, samples analyzed with the FTIR-ATR unit after demineralization were scanned again following the pH cycle. Data were processed in EssentialFTIR software (Operant LCC, U.S.A.). Phosphate and Amid I peak values were obtained in each spectrum after processing by baseline validation and normalization. The area under the phosphate/amide I peaks formed in the spectrum was calculated, and the changes in the mineral/matrix ratio were measured semi-quantitatively by comparing the values before and after the pH cycle [13].

Biofilm assays

Biofilm formation

After obtaining consent, unstimulated saliva samples were collected at least 1.5 h after eating, drinking, and tooth brushing from a periodontally healthy volunteer without caries. This method ensured bacterial adhesion on artificial root caries lesions and formation of the pellicle layer. The samples were centrifuged with a refrigerated centrifuge (3–18 K, Sigma, Germany) at 4 °C at 15,000 G/RCF (relative centrifugal force) for 15 min. The supernatant accumulated in the upper part of the tubes was sterilized by filtration with a 0.45 µm injector filter (Minisart, Sartorius, Germany). Sterile saliva was stored at −20°C [14].

Lactobacillus casei ATCC 4646 and *Streptococcus mutans* ATCC 25175 strains with international standards were used for bacterial biofilm experiments. Bacteria extracted from the stock (−80 ˚C) were inoculated on 5% sheep blood agar and incubated at 37 °C for 24 h. A bacterial suspension was prepared according to 0.5 McFarland standards (10^8CFU/ml) in 10 ml of Brain Heart Infusion (BHI) broth with 5% sucrose and diluted 100 fold. Thus, 1×10^6 bacteria were found in 1 ml of the suspension.

The discs were individually packaged and subjected to autoclave sterilization (121 °C for 15 min) ahead of microbiological assays [14]. Following the manufacturer's instructions, remineralization agents were applied to the sterilized specimens after the artificial caries lesion was created.

We used 24-well tissue culture plates to form biofilms. After a sample was placed in each well, 2 ml of saliva was added to cover the pellicle. The plates were then incubated in a shaker (MiniRocker MR-1, BioSan, Riga, Latvia) for 1 h at 37 °C.

Samples in saliva were washed with phosphate buffered saline (PBS) solution. After these steps, 200 µl of bacterial suspension and 1.6 ml of 5% sucrose BHI broth were added onto the samples placed in the new well.

Subsequently, the plates were placed in an anaerobic jar and incubated on a shaker at 37°C for 24 h [14].

Biofilm analysis

At the end of the incubation, the samples were taken from the plaques where bacterial growth was observed and washed three times with 5 ml of sterile saline to remove unadhered bacteria.

CLSM analysis

CLSM analysis was performed on seven samples from each group.

We prepared 0.4 µl/ml each of the A and B components of the Live/Dead Bacterial Viability Kit (Thermo Fisher Scientific, Molecular Probes, U.S.A.) in dimethyl sulfoxide (DMSO) used to stain the biofilm.

The prepared dye mixture was incubated in the dark for 15 min, leaving 20 µl on the materials in the plates. Stained samples were examined with CLSM (TCS SPE, Leica Microsystems, U.S.A.) at 488 and 532 nm at a magnification of 10x.

Image J program (National Institutes of Health, U.S.A.) was used to calculate the total and viable biomass (µm3/µm2) from the biofilm images obtained afterwards [15].

SEM analysis

To fix the biofilm, samples were kept in 4% formol for 40 min. After washing with water, it was dehydrated in ethylene glycol (10%, 25%, 50%, 75%, 90% for 20 min and 100% for 1 h). The dehydrated samples were coated in a coating device (SC7620 Sputter Coater, Quorum Technologies Ltd., U.K.) at 15 mA, 120 s, with an average of 1–2 nm Gold.

Conducted samples were examined by SEM (EVO LS10, Zeiss Microscopy, Germany) at 20 kV, 5000 × magnification [16].

Statistical analysis

Data were analyzed using the program SPSS 25.0 (SPSS Inc., Chicago IL, U.S.A). Kolmogorov–Smirnov test and Histogram graph were evaluated to determine whether or not the data showed normal distribution.

Kruskal–Wallis test was performed to compare the laser fluorescence values between agents. Bonferroni and Dunn's test was applied as post hoc analysis while evaluating the relationship of materials to each other considering differences between the measurements.

For repeated measure FTIR-ATR groups, pairwise comparison Wilcoxon Signed Rank test was used to determine the relationship between stages. When the difference between the groups was significant, Bonferroni test was applied as post hoc analysis. Kruskal–Wallis test was performed to compare CLSM results. Dunn's test was used as post hoc analysis while evaluating the relationship between the materials in the measurements that differed.

In all statistical analyses, $p < 0.05$ was considered significant.

Results

Laser fluorescence (DIAGNOdent)

In our study, after the application of remineralization agents on the samples with artificial root caries, changes on the surfaces were measured with the DIAGNOdent device. Sample surfaces were evaluated at the beginning (D1), after artificial caries formation (D2), and after pH cycle was applied (D3). Obtained data were analyzed statistically.

Mean ± SD LF values for Control (W), Proshield (P; 5% NaF), MI Varnish (M; 5% NaF + CPP-ACP), Clinpro (C; 5% NaF + TCP), Embrace (E; 5% NaF + CXP), and Riva Star (RS; SDF/KI) at baseline (D1), after demineralization (D2), and after pH cycling (D3) are shown in Fig. 2. Across groups, LF increased from D1 → D2 and declined at D3. From D2 → D3, RS showed the largest reduction (– 6.86; – 40.6%), M a modest reduction (– 1.90; – 9.9%), P showed no change, whereas C and E exhibited slight increases (~ + 6.2% each); Control increased by + 33.2%. At D3, all varnish groups differed significantly from Control, indicating lower LF in the experimental groups, and RS also differed from each of the other varnish groups, yielding the lowest LF at D3.

FTIR-ATR analysis

Figure 3 shows representative FTIR-ATR spectra for W (Control), P (NaF), M (CPP-ACP), C (TCP), E (CXP), and RS (SDF/KI) before (top) and after (bottom) pH cycling. The spectra illustrate typical band positions and qualitative changes in the ν3-phosphate region (≈1200–900 cm^{-1}, peak ≈1030 cm^{-1}). Consistent with those statistics, varnish-treated groups generally retained higher post-cycling phosphate/amide I values than Control (i.e., greater relative mineral preservation). In the RS group, additional post-cycling features were evident—most notably a weak C = O stretch near ≈1735–1740 cm^{-1} and a subtle shoulder within the ν3-phosphate envelope around ≈1090–1095 cm^{-1}—suggestive of chemical interaction with dentin. We note that Fig. 3 panels are exemplars and may not reflect group means in magnitude.

Group-wise phosphate/amide I (mineral/matrix) mean ± SD ratios before → after pH cycling were: Control 0.77 ± 0.54 → 0.27 ± 0.10 (Δ – 0.500 ± 0.447; p = 0.0625); NaF (P) 1.32 ± 0.57 → 0.67 ± 0.55 (Δ – 0.642 ± 0.100; p = 0.0625); CPP-ACP (M) 1.45 ± 0.65 → 1.08 ± 0.68 (Δ – 0.366 ± 0.239; p = 0.0625); TCP (C) 0.72 ± 0.22 → 0.35 ± 0.20 (Δ – 0.373 ± 0.186; p = 0.0625); CXP (E) 1.74 ± 0.16 → 0.39 ± 0.26 (Δ – 1.353 ± 0.255; p = 0.0625) The RS (SDF/KI) group was

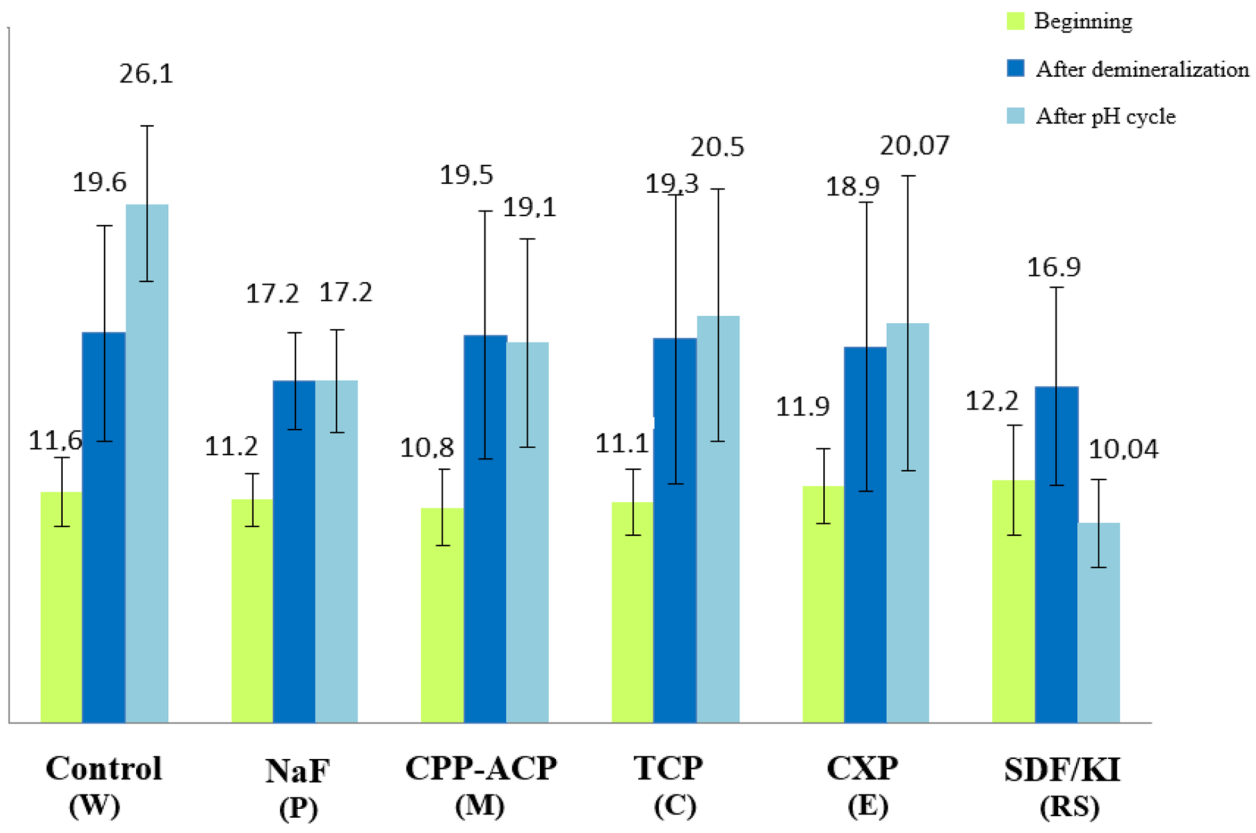

Fig. 2 The mean and standard deviation values of groups obtained by laser fluorescence

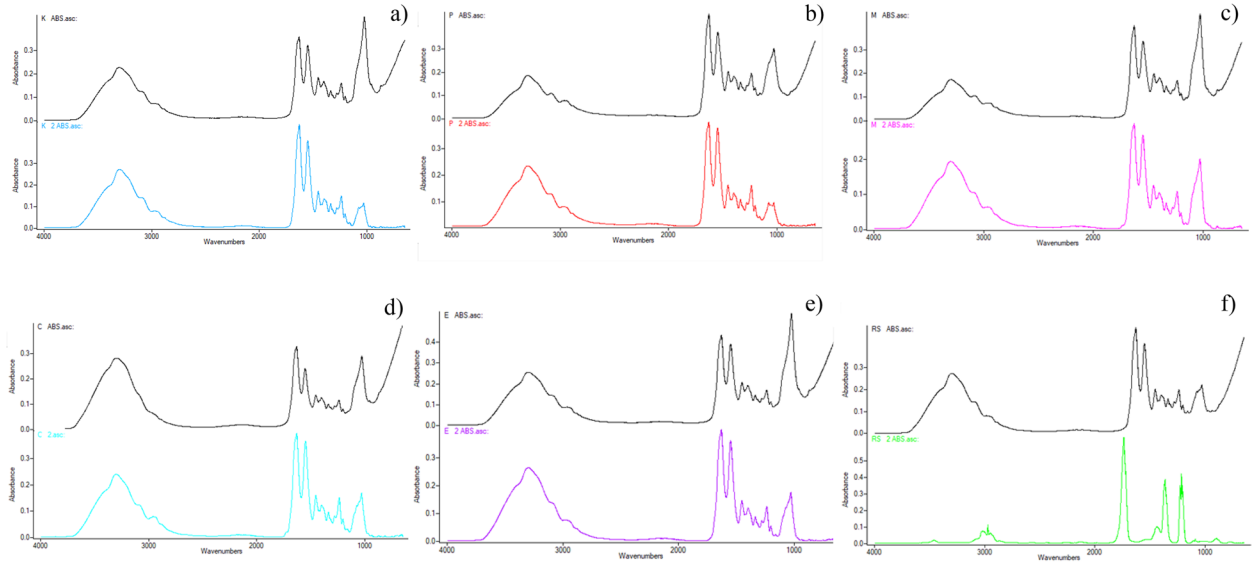

Fig. 3 Representative FTIR-ATR spectra (not group means) for **a**) Control (W), **b**) NaF (P), **c**) CPP-ACP (M), **d**) TCP (C), **e**) CXP (E), **f**) SDF/KI (RS) before (top) and after (bottom) pH cycling. Spectra are shown to illustrate band positions and qualitative trends; quantitative phosphate/amide I ratios with statistical evaluation are given in the text. In RS, post-cycling features in the 1100–1000 cm^{-1} region and a weak shoulder near ≈1735–1740 cm^{-1} are evident

not ratio-quantified due to reference-band limitations; thus, for RS we report qualitative spectral changes only.

Post-cycling phosphate/amide I ratios tended to be higher in all varnish groups than Control, and no significant differences were detected among varnish groups in multiple comparisons ($p > 0.05$).

Overall, FTIR-ATR findings support greater mineral preservation in varnish groups relative to Control, while

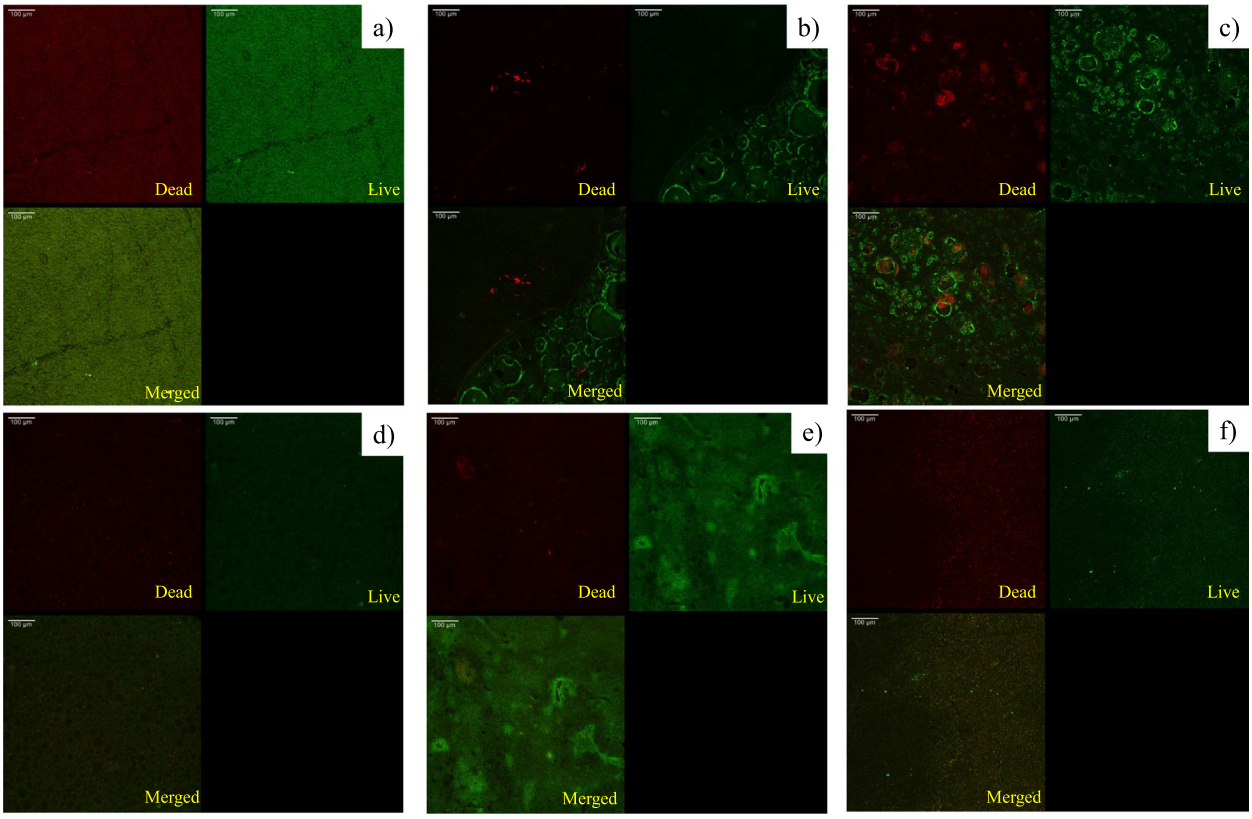

Fig. 4 CLSM images of dual-species biofilms (*Streptococcus mutans* + *Lactobacillus casei*): **a**) Control (W), **b**) NaF (P), **c**) CPP-ACP (M), **d**) TCP (C), **e**) CXP (E), **f**) SDF/KI (RS). Within each panel, tiles represent Dead (red), Live (green), and Merged (red + green) views (lower-right tile left blank per export). Dead cells = red; live cells = green. Scale bar: 100 µm

Table 2 Total biomass and live biomass mean and standard deviation

	Total biomass (µm3/µm2)	Live biomass (µm3/µm2)
Control (W)	255.33 ± 41.32^{A}	119.33 ± 19.21^{a}
NaF (P)	71.75 ± 23.22^{E}	14.09 ± 4.70^{e}
CPP-ACP (M)	117.76 ± 16.56^{CD}	36.03 ± 4.13^{d}
TCP (C)	109.03 ± 27.59^{DE}	47.45 ± 17.31^{cd}
CXP (E)	172.40 ± 36.67^{BC}	51.37 ± 9.55^{c}
SDF/KI (RS)	160.21 ± 25.70^{B}	77.45 ± 12.73^{b}

*Different superscript letters within the same column indicate statistically significant differences ($p < 0.05$). Groups sharing at least one letter are not significantly different. Capital letters denote comparisons for total biomass; lowercase letters denote comparisons for live biomass

SDF/KI shows distinct post-cycling features consistent with dentin–silver chemistry.

CLSM analysis

Figure 4 presents CLSM images of *S. mutans/L. casei* biofilms. Table 2 lists group-wise mean ± SD for total biomass and live biomass. Numerically, total biomass ($\mu m^3/\mu m^2$; mean ± SD) was: Control 255.33 ± 41.32; NaF 71.75 ± 23.22; CPP-ACP 117.76 ± 16.56; TCP 109.03 ± 27.59; CXP 172.40 ± 36.67; SDF/KI 160.21 ± 25.70. Live biomass ($\mu m^3/\mu m^2$; mean ± SD) was: Control 119.33 ± 19.21; NaF 14.09 ± 4.70; CPP-ACP 36.03 ± 4.13; TCP 47.45 ± 17.31; CXP 51.37 ± 9.55; SDF/KI 77.45 ± 12.73. Among varnishes, NaF yielded the lowest total and live biomass; groups sharing the same superscript letter in Table 2 did not differ statistically (Kruskal–Wallis with Dunn's post-hoc).

CLSM quantification shows substantial biofilm suppression across varnishes relative to Control, with NaF yielding the lowest total and live biomass among treatments.

SEM analysis

SEM images of *S. mutans* and *L. casei* biofilms formed on the surface of the samples at X5000 magnification are shown in Fig. 5.

SEM imagery revealed that while biofilm consisting of common cocci and rods was very clear in the control group, varnish residues were mostly observed in the study groups and a clear biofilm could not be determined.

Discussion

In this study, across an aggressive pH-cycling model that simulates frequent acid challenges, SDF/KI produced the lowest post-cycle laser fluorescence values

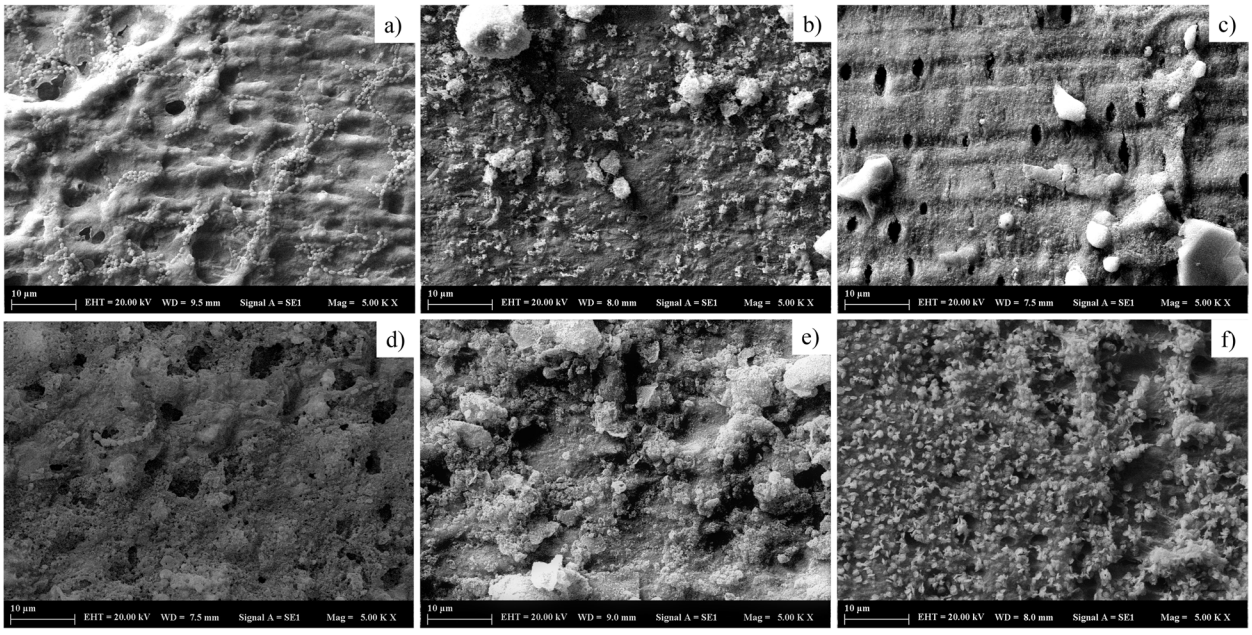

Fig. 5 SEM images of *S. mutans* and *L. casei* biofilms formed on the surface of **a**) Control (W), **b**)NaF (P), **c**) CPP-ACP (M), **d**) TCP (C), **e**) CXP (E), **f**) SDF/KI (RS) samples at X5000 magnification

(DIAGNOdent), indicating the strongest inhibition of demineralization among the tested agents. Conventional 5% NaF varnish also protected root dentin relative to the water control, whereas adding CPP-ACP, TCP, or CXP to NaF did not improve outcomes beyond NaF alone in this setting. FTIR-ATR corroborated these trends: varnish groups other than SDF/KI retained higher phosphate/amide I (mineral/matrix) ratios than control after cycling, while spectra from SDF/KI showed additional bands consistent with chemical modifications of the organic phase. Confocal microscopy and SEM suggested reduced biofilm accumulation on treated surfaces compared with control; however, differences among varnishes were less consistent and should be interpreted cautiously given the in-vitro model and imaging-based quantification.

Fluoride varnishes remain a mainstay for caries prevention, with 5% sodium fluoride (NaF) the most widely used formulation. Recent variants incorporate additional remineralization agents—such as CPP-ACP (Recaldent™), functionalized β-TCP (fTCP; Clinpro™), and xylitol-coated calcium-phosphate (CXP™; Embrace™)—to enhance ion availability at the tooth–biofilm interface. These systems aim to deliver Ca/PO_4 reservoirs and stabilize ACP phases that bind to hydroxyapatite and diffuse within biofilm [17–19]. Silver diamine fluoride (SDF) provides both fluoride and silver ions and is effective in preventing/arresting caries, but causes discoloration; applying potassium iodide (KI) in a two-step SDF/KI protocol has been proposed to mitigate staining [20, 21]. While many evaluations target enamel, the performance of these formulations on cementum/dentin in root caries remains less clear, motivating the present comparison.

Artificial lesion chemical models are widely used to test remineralization agents owing to their standardization, cost-effectiveness, and repeatability [22]. Substrate characteristics are critical: whereas coronal initial lesions often retain a hypermineralized surface layer, root caries frequently lack this layer; when cementum persists, a thin superficial hypermineralized cementum may remain [23]. Because natural root lesions are heterogeneous and difficult to standardize [24], prior work recommends removing/abrading cementum to improve reproducibility [25]; we followed this approach to standardize baseline demineralization across specimens. Rather than a traditional net-remineralization paradigm—where prolonged neutral/alkaline exposure can yield recovery even in controls [26, 27]—we employed an aggressive, intermittent pH-cycling scheme [11] to emulate repeated daily acid attacks and to emphasize inhibition capacity. Taken together, these model choices contextualize our results: under frequent acid challenge, SDF/KI outperformed all comparators, NaF provided baseline protection, and adding CPP-ACP/fTCP/CXP conferred no additional benefit.

Our LF findings place SDF/KI as the most effective option for protecting root dentin under repeated acidic episodes, aligning with the well-documented remineralization/anti-demineralization efficacy of SDF per se on enamel and dentin [28–30]. Its superiority over NaF-based varnishes is biologically plausible: concurrent availability of F^- and Ag^+ can generate CaF_2-like

reservoirs and silver compounds (e.g., Ag_3PO_4) that harden lesions and may limit collagen degradation. In contrast, 5% NaF behaved as a broadly preventive baseline [31]. For NaF-additive systems, our data show no incremental benefit of CPP-ACP, fTCP, or CXP over NaF under aggressive cycling. This pattern fits prior evidence: CPP-ACP can enhance remineralization on root dentin [32–34] yet often does not outperform NaF in pH-cycling models; fTCP tends to exceed control but not NaF—possibly because highly mineralized surface precipitates impede subsurface ion diffusion [9], and available CXP data are sparse, with enamel studies showing no advantage over NaF alone [27]. Taken together, these comparisons explain why, in our inhibition-focused model, SDF/KI outperformed all comparators, whereas NaF ≈ NaF + additives**.**

Although KI is intended to mitigate SDF-associated discoloration, we still observed visible darkening on some specimens, a phenomenon commonly attributed to the precipitation and photoreduction of silver compounds (e.g., $Ag^+/Ag_3PO_4/AgI$) to metallic silver (Ag^0) [35]. Consistent with compositional changes during cycling, the ν3-phosphate region (≈1200–900 cm^{-1} peak ≈1030 cm^{-1}) showed post-cycling attenuation to varying extents across groups; quantitative phosphate/amide I values are reported in results and should be used for inference. In the SDF/KI group, additional post-cycling features were evident—most prominently a weak C = O stretch near ~ 1738 cm^{-1} and a subtle shoulder within the ν3-phosphate envelope around ~ 1090–1095 cm^{-1}. We interpret these bands cautiously as consistent with matrix-level modifications (e.g., carbonyl formation within dentin collagen) and the presence of silver–phosphate/fluoride reaction products via SDF/KI chemistry (e.g., Ag_3PO_4 and CaF_2), rather than changes in apatite content alone [29, 30]. Because reference bands could not be robustly defined for SDF/KI, we did not compute phosphate/amide I ratios for this group; instead, we report these spectral changes descriptively, noting that carbonyl bands in the ~ 1730–1740 cm^{-1} range have also been observed in root dentin after certain sealer applications [36], supporting the plausibility of organic-phase C = O signals. Taken together, these findings indicate a distinct chemical trajectory for SDF/KI compared with fluoride-only varnishes.

Fluoride at sufficient concentrations perturbs carbohydrate metabolism and sugar transport in cariogenic bacteria [37]. Prior work suggests CPP-ACP can suppress *Streptococcus mutans* biofilms [38, 39], whereas fTCP often shows biofilm effects comparable to NaF [15]. Evidence for CXP remains limited and mixed [40, 41]. For SDF/KI, several studies report reductions in *S. mutans* counts and increased dentin resistance, though the incremental contribution of KI over SDF alone is inconsistent [42–48]. Because multispecies biofilms are typically more tolerant [49], dentin-block data are informative: SDF suppresses dual/multispecies consortia containing *S. mutans* and *Lactobacillus* spp. [50], and SDF/KI often reduces colony-forming units (CFU) to a similar extent as SDF alone [51]. In our single-donor, dual-species model (*S. mutans* and *L. casei*), CLSM and SEM likewise showed reductions versus control but no consistent superiority among NaF-based varnishes—differences that likely reflect variation in residual surface films, local fluoride/silver availability, and the limits of imaging-only quantification. Future work should incorporate multi-donor polymicrobial consortia and complementary endpoints (e.g., CFU, qPCR, EPS assays) to triangulate imaging-based metrics.

It is clear that the different experimental designs and analysis methods used in all these studies have a direct impact on the results. In addition, when our study is evaluated within itself, it is thought that the effects of the varnishes used on the biofilm, as well as the film thicknesses and adhesion abilities of the agents on the tooth surfaces, may affect the results.

Within the limits of this in-vitro model, SDF/KI appears the most robust option for arresting or protecting high-risk root surfaces, whereas NaF alone remains reasonable for general prevention when aesthetic concerns predominate. Our findings do not support a routine advantage of adding CPP-ACP, TCP, or CXP to NaF for root dentin under frequent acid challenges. Given the known staining risk with silver agents—even when mitigated with KI—clinical selection should weigh caries risk, lesion visibility, and patient priorities.

This study has several limitations. First, quantification based on CLSM fluorescence may be affected by biofilm thickness and imaging parameters (e.g., brightness, contrast, white balance). Second, the experiment was short-term and conducted in vitro, which cannot fully reproduce the complexity of the oral environment. Third, only one biofilm model and a limited set of agents were assessed. These factors temper generalizability to clinical outcomes.

SDF/KI most effectively inhibited demineralization on root dentin under frequent acid stress; NaF provided meaningful but lesser protection; NaF combined with CPP-ACP, TCP, or CXP did not surpass NaF alone. Future studies should (1) compare SDF vs. SDF/KI head-to-head for both hard-tissue and staining endpoints (objective colorimetry), (2) integrate ion-release kinetics and silver deposition mapping (e.g., EDX/μ-XRF), (3) deploy polymicrobial, multi-donor biofilms and longer cycling, and (4) validate LF/FTIR readouts against transverse microradiography or microhardness for lesion-level calibration.

Conclusion

In this in-vitro pH-cycling model of root dentin, SDF/KI provided the strongest inhibition of demineralization, while 5% NaF offered meaningful baseline protection. Combining NaF with CPP-ACP, TCP, or CXP did not yield incremental benefits over NaF alone under frequent acid challenges. Because experiments were short-term and laboratory-based, clinical extrapolation should be cautious; trials that jointly assess hard-tissue outcomes and objective color change are warranted.

Abbreviations

ACP	Amorphous calcium phosphate
ATCC	American Type Culture Collection
ATR	Attenuated total reflectance
BHI	Brain Heart Infusion
$CaCl_2$	Calcium chloride
CFU	Colony-forming unit
CLSM	Confocal laser scanning microscopy
CPP	Casein phosphopeptide
CPP-ACP	Casein phosphopeptide–amorphous calcium phosphate
CXP	Xylitol-coated calcium phosphate
D1, D2, D3	DIAGNOdent fluorescence values: baseline (D1), after demineralization (D2), after pH cycling (D3)
DMSO	Dimethyl sulfoxide
fTCP	Functionalized β-tricalcium phosphate
FTIR	Fourier transform infrared spectroscopy
FTIR-ATR	Fourier transform infrared spectroscopy with attenuated total reflectance
HEPES	4-(2-Hydroxyethyl)-1-piperazineethanesulfonic acid
KCl	Potassium chloride
KH_2PO_4	Monopotassium phosphate
KI	Potassium iodide
LF	Laser fluorescence
NaF	Sodium fluoride
PBS	Phosphate-buffered saline
RCF	Relative centrifugal force
SDF	Silver diamine fluoride
SDF/KI	Silver diamine fluoride/potassium iodide
SD	Standard deviation
SEM	Scanning electron microscopy
SPSS	Statistical Package for the Social Sciences
TCP	Tricalcium phosphate
β-TCP	Beta-tricalcium phosphate
W	Sterile deionized water (control)
P	Proshield Varnish (5% NaF)
M	MI Varnish (5% NaF + CPP-ACP)
C	Clinpro (5% NaF + TCP)
E	Embrace Varnish (5% NaF + CXP)
RS	Riva Star (SDF/KI)

Acknowledgements

The authors thank Assoc. Prof. Canan Kücükgergin for technical support during demineralization and remineralization solutions preparation, Emine Mutlu for biofilm formation, Karolin Yanar for assistance with saliva centrifugation, Zeynep Ozturk for statistical support, and Martin Duncan for language proofreading. This article is based on the corresponding author's specialization thesis

Authors' contributions

M.S.:Conceptualization, Data curation, Investigation, Methodology, Software, Writing-Original Draft D.E.:Funding acquisition, Project administration, Supervision, Writing-review & editing N.T.:Conceptualization, Data curation, Investigation, Methodology, Supervision. All authors reviewed the manuscript.

Funding

The present work was supported by the Research Fund of Istanbul University (Project No. 36623). The English language editing fee was covered by Istanbul Kent University.

Data availability

The datasets generated and analyzed during this study are available from the corresponding author upon reasonable request. All essential data supporting the findings are included within the manuscript.

Declarations

Ethics approval and consent to participate

All procedures in this study were conducted in accordance with the Declaration of Helsinki. As only animal by-products were used and no procedures were performed on live animals, formal ethical approval was not required. Ethical approval for the saliva sample was obtained from the Istanbul University Faculty of Dentistry, Non-Interventional Clinical Research Ethics Committee (File no: 2019/63; Decision no: 88; Date: 11/07/2019). Informed consent was obtained from the single donor who provided the saliva sample.

Consent for publication

Not applicable.

Competing interests

The authors declare no competing interests.

Received: 19 July 2025 / Accepted: 4 December 2025
Published online: 18 December 2025

References

1. Pentapati KC, Siddiq H, Yeturu SK. Global and regional estimates of the prevalence of root caries – systematic review and meta-analysis. Saudi Dent J. 2019;31(1):3–15. https://doi.org/10.1016/j.sdentj.2018.11.008.
2. Oliveira BH, Cunha-Cruz J, Rajendra A, Niederman R. Controlling caries in exposed root surfaces with silver diamine fluoride: a systematic review with meta-analysis. J Am Dent Assoc. 2018;149(8):671-679.e1. https://doi.org/10.1016/j.adaj.2018.03.028.
3. Bosshardt DD, Selvig KA. Dental cementum: the dynamic tissue covering of the root. Periodontol 2000. 1997;13(1):41–75. https://doi.org/10.1111/j.1600-0757.1997.tb00095.x.
4. Abou Neel E, Aljabo A, Strange A, et al. Demineralization&remineralization dynamics in teeth and bone. Int J Nanomedicine. 2016;11:4743–63. https://doi.org/10.2147/IJN.S107624.
5. Cai J, Palamara J, Manton D, Burrow M. Status and progress of treatment methods for root caries in the last decade: a literature review. Aust Dent J. 2018;63(1):34–54. https://doi.org/10.1111/adj.12550.
6. Demir G. Current Overview of Remineralization Materials and Technologies. (Remineralizasyon materyalleri ve teknolojilerine güncel bakış.). Yeditepe Dent J. 2019;16(1):81–94. https://doi.org/10.5505/yeditepe.2020.16023.
7. Wierichs RJ, Meyer-Lueckel H. Systematic review on noninvasive treatment of root caries lesions. J Dent Res. 2015;94(2):261–71. https://doi.org/10.1177/0022034514557330.
8. Secilmis A, Dilber E, Gokmen F, Ozturk N, Telatar T. Effects of storage solutions on mineral contents of dentin. J Dent Sci. 2011;6(4):189–94. https://doi.org/10.1016/j.jds.2011.09.001.
9. Wierichs RJ, Stausberg S, Lausch J, Meyer-Lueckel H, Esteves-Oliveira M. Caries-preventive effect of NaF, NaF plus TCP, NaF plus CPP-ACP, and SDF varnishes on sound dentin and artificial dentin caries *in vitro*. Caries Res. 2018;52(3):199–211. https://doi.org/10.1159/000484483.
10. Cai J, Burrow MF, Manton DJ, Tsuda Y, Sobh EG, Palamara JEA. Effects of silver diamine fluoride/potassium iodide on artificial root caries lesions with adjunctive application of proanthocyanidin. Acta Biomater. 2019;88:491–502. https://doi.org/10.1016/j.actbio.2019.02.020.
11. Mei ML, Ito L, Cao Y, Li QL, Lo ECM, Chu CH. Inhibitory effect of silver diamine fluoride on dentine demineralisation and collagen degradation. J Dent. 2013;41(9):809–17. https://doi.org/10.1016/j.jdent.2013.06.009.
12. Varma V, Hegde KS, Bhat SS, Sargod SS, Rao HA. Comparative evaluation of remineralization potential of two varnishes containing CPP–ACP and

tricalcium phosphate: an *in vitro* study. Int J Clin Pediatr Dent. 2019;12(3):233–6. https://doi.org/10.5005/jp-journals-10005-1629.
13. Jiang T, Ma X, Wang Y, Zhu Z, Tong H, Hu J. Effects of hydrogen peroxide on human dentin structure. J Dent Res. 2007;86(11):1040–5. https://doi.org/10.1177/154405910708601104.
14. Kurt A, Cilingir A, Bilmenoglu C, Topcuoglu N, Kulekci G. Effect of different polishing techniques for composite resin materials on surface properties and bacterial biofilm formation. J Dent. 2019;90:103199. https://doi.org/10.1016/j.jdent.2019.103199.
15. Yu OY, Zhao IS, Mei ML, Lo ECM, Chu CH. Effect of silver nitrate and sodium fluoride with tri-calcium phosphate on *Streptococcus mutans* and demineralised dentine. Int J Mol Sci. 2018;19(5):1288. https://doi.org/10.3390/ijms19051288.
16. Yao L, Li Y, Fu D, Ji M, Zou L, Jiang L. Comparison of TiF4, CPP-ACP, and NaF in preventing demineralization in irradiated bovine enamel and dentin *in vitro*. J Appl Oral Sci. 2025. https://doi.org/10.1590/1678-7757-2024-0524.
17. Nongonierma AB, FitzGerald RJ. Biofunctional properties of caseinophosphopeptides in the oral cavity. Caries Res. 2012;46(3):234–67. https://doi.org/10.1159/000338381.
18. Karlinsey RL, Pfarrer AM. Fluoride plus functionalized β-TCP. Adv Dent Res. 2012;24(2):48–52. https://doi.org/10.1177/0022034512449463.
19. Milburn JL, Henrichs LE. Substantive Fluoride Release from a New Fluoride Varnish Containing CXP. Dentistry. 2015;5(12). https://doi.org/10.4172/2161-1122.1000350.
20. Zhao IS, Gao SS, Hiraishi N, et al. Mechanisms of silver diamine fluoride on arresting caries: a literature review. Int Dent J. 2018;68(2):67–76. https://doi.org/10.1111/idj.12320.
21. Knight G, McIntyre J, Craig G, Mulyani, Zilm P, Gully N. An in vitro model to measure the effect of a silver fluoride and potassium iodide treatment on the permeability of demineralized dentine to Streptococcus mutans. Aust Dent J. 2005;50(4):242–245. https://doi.org/10.1111/j.1834-7819.2005.tb00367.x.
22. Yu OY, Mei ML, Zhao IS, Lo ECM, Chu CH. Effects of fluoride on two chemical models of enamel demineralization. Materials. 2017;10(11):1245. https://doi.org/10.3390/ma10111245.
23. Nyvad B, Fejerskov O. Root surface caries: clinical, histopathological and microbiological features and clinical implications. Int Dent J. 1982;32(4):311–26.
24. Arnold WH, Heidt BA, Kuntz S, Naumova EA. Effects of fluoridated milk on root dentin remineralization. PLoS One. 2014;9(8):e108199. https://doi.org/10.1371/journal.pone.0108199.
25. Smith PW, Preston KP, Higham SM. Development of an in situ root caries model. A in vitro investigations. J Dent. 2005;33(3):253–67. https://doi.org/10.1016/j.jdent.2004.10.020.
26. Tuloglu N, Bayrak S, Tunc ES, Ozer F. Effect of fluoride varnish with added casein phosphopeptide-amorphous calcium phosphate on the acid resistance of the primary enamel. BMC Oral Health. 2016;16(1):103. https://doi.org/10.1186/s12903-016-0299-4
27. Mohd Said SNB, Ekambaram M, Yiu CKY. Effect of different fluoride varnishes on remineralization of artificial enamel carious lesions. Int J Paediatr Dent. 2017;27(3):163–73. https://doi.org/10.1111/ipd.12243.
28. Vinod D, Gopalakrishnan A, Subramani SM, Balachandran M, Manoharan V, Joy A. A comparative evaluation of remineralizing potential of three commercially available remineralizing agents: an in vitro study. Int J Clin Pediatr Dent. 2020;13(1):61–5. https://doi.org/10.5005/jp-journals-10005-1715.
29. Chu CH, Mei L, Seneviratne CJ, Lo ECM. Effects of silver diamine fluoride on dentine carious lesions induced by *Streptococcus mutans* and *Actinomyces naeslundii* biofilms. Int J Paediatr Dent. 2012;22(1):2–10. https://doi.org/10.1111/j.1365-263X.2011.01149.x.
30. Yu OY, Zhao IS, Mei ML, Lo ECM, Chu CH. Caries-arresting effects of silver diamine fluoride and sodium fluoride on dentine caries lesions. J Dent. 2018;78:65–71. https://doi.org/10.1016/j.jdent.2018.08.007.
31. Marinho VC, Worthington HV, Walsh T, Clarkson JE. Fluoride varnishes for preventing dental caries in children and adolescents. Cochrane Database Syst Rev. 2013. https://doi.org/10.1002/14651858.CD002279.pub2.
32. Mohammadi N, Rikhtegaran S, Kimyai S, et al. The effect of photodynamic therapy and casein phosphopeptide-amorphous calcium phosphate (CPP-ACP) on the remineralization rate of non-cavitated root: an in-vitro study. Maedica J Clin Med. 2019;14(4):357–62. https://doi.org/10.26574/maedica.2019.14.4.357.
33. Rahiotis C, Vougiouklakis G. Effect of a CPP-ACP agent on the demineralization and remineralization of dentine *in vitro*. J Dent. 2007;35(8):695–8. https://doi.org/10.1016/j.jdent.2007.05.008.
34. Salem G, Shalaby HA, Khafagi MG. Efficiency of two remineralization pastes on demineralized enamel and dentine of deciduous teeth. Egypt Dent J. 2015;61:4623–31.
35. Peng JJY, Botelho MG, Matinlinna JP. Silver compounds used in dentistry for caries management: a review. J Dent. 2012;40(7):531–41. https://doi.org/10.1016/j.jdent.2012.03.009.
36. Neelakantan P, Sharma S, Shemesh H, Wesselink PR. Influence of irrigation sequence on the adhesion of root canal sealers to dentin: a Fourier transform infrared spectroscopy and push-out bond strength analysis. J Endod. 2015;41(7):1108–11. https://doi.org/10.1016/j.joen.2015.02.001.
37. Mei ML, Li Q, Chu CH, Lo EM, Samaranayake LP. Antibacterial effects of silver diamine fluoride on multi-species cariogenic biofilm on caries. Ann Clin Microbiol Antimicrob. 2013;12(1):4. https://doi.org/10.1186/1476-0711-12-4.
38. Attiguppe P, Malik N, Ballal S, Naik SV. CPP–ACP and fluoride: a synergism to combat caries. Int J Clin Pediatr Dent. 2019;12(2):120–5. https://doi.org/10.5005/jp-journals-10005-1608.
39. Sionov RV, Tsavdaridou D, Aqawi M, Zaks B, Steinberg D, Shalish M. Tooth mousse containing casein phosphopeptide-amorphous calcium phosphate prevents biofilm formation of *Streptococcus mutans*. BMC Oral Health. 2021;21(1):136. https://doi.org/10.1186/s12903-021-01502-6.
40. Bahador A, Lesan S, Kashi N. Effect of xylitol on cariogenic and beneficial oral streptococci: a randomized, double-blind crossover trial. Iran J Microbiol. 2012;4(2):75–81.
41. Erkmen Almaz M, Akbay Oba A. Antibacterial activity of fluoride varnishes containing different agents in children with severe early childhood caries: a randomised controlled trial. Clin Oral Investig. 2020;24(6):2129–36. https://doi.org/10.1007/s00784-020-03300-w.
42. Hamama H, Yiu C, Burrow M. Effect of silver diamine fluoride and potassium iodide on residual bacteria in dentinal tubules. Aust Dent J. 2015;60(1):80–7. https://doi.org/10.1111/adj.12276.
43. Knight GM, McIntyre JM, Craig GG, Mulyani, Zilm PS, Gully NJ. Inability to form a biofilm of Streptococcus mutans on silver fluoride- and potassium iodide-treated demineralized dentin. Quintessence Int. 2009;40(2):155-161.
44. Abdullah N, Al Marzooq F, Mohamad S, et al. The antibacterial efficacy of silver diamine fluoride (SDF) is not modulated by potassium iodide (KI) supplements: a study on in-situ plaque biofilms using viability real-time PCR with propidium monoazide. PLoS One. 2020;15(11):e0241519. https://doi.org/10.1371/journal.pone.0241519.
45. Takahashi M, Matin K, Matsui N, et al. Effects of silver diamine fluoride preparations on biofilm formation of *Streptococcus mutans*. Dent Mater J. 2021;40(4):911–7. https://doi.org/10.4012/dmj.2020-341.
46. Karched M, Ali D, Ngo H. In vivo antimicrobial activity of silver diammine fluoride on carious lesions in dentin. J Oral Sci. 2019;61(1):19–24. https://doi.org/10.2334/josnusd.17-0366.
47. Vinson LA, Gilbert PR, Sanders BJ, Moser E, Gregory RL. Silver diamine fluoride and potassium iodide disruption of *in vitroStreptococcus mutans* biofilm. J Dent Child (Chic). 2018;85(3):120–4.
48. Tiba AA, Tiba A, Horvath F, et al. Effects of a two-step silver diamine fluoride varnish on shear bond strength of restorations, dentin and enamel hardness, and biofilm formation. Mil Med. 2024;189(3–4):592–7. https://doi.org/10.1093/milmed/usac216.
49. Cowan SE, Gilbert E, Liepmann D, Keasling JD. Commensal interactions in a dual-species biofilm exposed to mixed organic compounds. Appl Environ Microbiol. 2000;66(10):4481–5. https://doi.org/10.1128/AEM.66.10.4481-4485.2000.
50. Mei ML, Chu CH, Low KH, Che CM, Lo ECM. Caries arresting effect of silver diamine fluoride on dentine carious lesion with S. mutans and L. acidophilus dual-species cariogenic biofilm. Med Oral Patol Oral Cir Bucal. Published online 2013:e824-e831. https://doi.org/10.4317/medoral.18831.
51. Kim H, Park H, Lee J, Lee S. Surface roughness of dentin and formation of early cariogenic biofilm after silver diamine fluoride and potassium iodide application. J Korean Acad Pediatr Dent.. 2022;49(2):140–8. https://doi.org/10.5933/jkapd.2022.49.2.140.

Publisher's Note